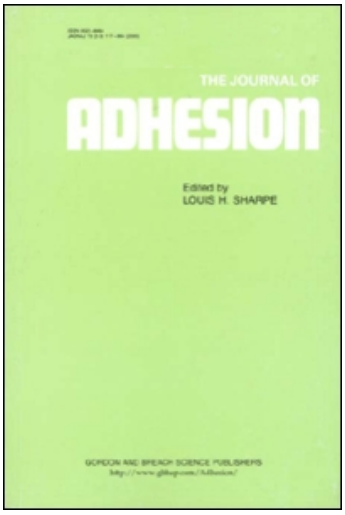

The Journal of Adhesion
Publication details, including instructions for authors and subscription information:
http://www.informaworld.com/smpp/title~content=t713453635

CRACK GROWTH OF STRUCTURAL ADHESIVE JOINTS IN HUMID ENVIRONMENTS

C. F. Korenberg[a]; A. J. Kinloch[a]; J. F. Watts[b]
[a] Department of Mechanical Engineering, London, UK [b] The Surface Analysis Laboratory, Guildford, Surrey, UK

Online publication date: 18 June 2010

To cite this Article Korenberg, C. F. , Kinloch, A. J. and Watts, J. F.(2004) 'CRACK GROWTH OF STRUCTURAL ADHESIVE JOINTS IN HUMID ENVIRONMENTS', The Journal of Adhesion, 80: 3, 169 — 201
To link to this Article: DOI: 10.1080/00218460490279233
URL: http://dx.doi.org/10.1080/00218460490279233

The Journal of Adhesion, 80: 169–201, 2004

ISSN: 0021-8464 print/1545-5823 online
DOI: 10.1080/00218460490279233

Taylor & Francis
Taylor & Francis Group

CRACK GROWTH OF STRUCTURAL ADHESIVE JOINTS IN HUMID ENVIRONMENTS

C. F. Korenberg
A. J. Kinloch
Department of Mechanical Engineering,
Imperial College London, Exhibition Road, London, UK

J. F. Watts
The Surface Analysis Laboratory,
School of Engineering, University of Surrey,
Guildford, Surrey, UK

The adhesive fracture energy, G_c, of aluminium alloy and steel joints bonded with a rubber-toughened epoxy adhesive has been measured using monotonically loaded tests. Such tests have been conducted at different levels of relative humidity, and two surface pretreatments have been employed for the substrates prior to bonding: a simple grit-blast and degrease (GBD) pretreatment or a silane primer (GBS) pretreatment. When G_c was plotted against the crack velocity, three regions of fracture behaviour could be distinguished. At low rates of displacement the crack grew in a stable manner, visually along the interface, and relatively low crack velocities could be readily measured. This was termed "Region I," and here the value of the adhesive fracture energy was relatively low and decreased steadily as the relative humidity was increased. On the other hand, at relatively high rates of displacement the crack grew in a stick-slip manner mainly cohesively in the adhesive layer at approximately 20 km/min. This was termed "Region III," and here the value of G_c was relatively high and independent of the relative humidity. In this region the crack was considered to grow faster than the water molecules were able to reach the crack tip, which explains the independence of G_c upon the test environment. In between Region I and Region III, a transition region was

Received 10 July 2003; in final form 28 October 2003.

Present address of C. F. Korenberg is Department of Conservation, Documentation and Science, The British Museum, London WC1B 3DG, UK. E-mail: a.kinloch@imperial.ac.uk

The authors would like to thank Dr. D. Tod (QinetiQ) for financial support for Dr. C. Korenberg and Mr. K. T. Tan and Dr. V. Tropsa (Imperial College London) for helpful discussions. They also wish to thank Mr. Steve Greaves of the University of Surrey for conducting the XPS studies.

Address correspondence to A. J. Kinloch, Department of Mechanical Engineering, Imperial College London, Exhibition Road, London SW7 2AZ, UK. E-mail: a.kinloch@imperial.ac.uk

observed, which was designated "Region II." The major effect of the GBS pretreatment, compared with GBD pretreatment, was to increase the value of G_c both in Regions I and III, although the presence of the silane primer had the greater effect in Region I.

Keywords: Accelerated testing; Durability; Environmental attack; Fracture mechanics, Structural adhesives

INTRODUCTION

The use of structural adhesives offers many advantages when compared with other more traditional joining methods such as welding, riveting, and mechanical fasteners [1]. However, as with any technology, there are some potential disadvantages associated with the use of adhesives. In particular, adhesive joints may suffer environmental attack when exposed to relatively hot and humid environments. The development of a sound accelerated-ageing test method to assess the susceptibility of an adhesive system (*i.e.*, the adhesive/primer (if any)/substrate and substrate surface pretreatment in combination) to such attack would represent a significant advance, especially if such tests could be completed in a relatively short time scale [2].

The aim of a sound and meaningful accelerated ageing test must be to accelerate the mechanisms of attack seen during the service-life of the bonded joint and not to induce misleading and irrelevant mechanisms. For example, it is well known that to accelerate the rate of environmental attack it is not possible simply to raise the temperature of the environment, since unrealistically high test temperatures will indeed change the mechanisms of attack. One method of accelerating the rate of attack which has recently been explored in detail by Kinloch and coworkers (*e.g.*, Jethwa and Kinloch [3]) has been the use of cyclic fatigue tests, using a fracture mechanics approach, conducted in aqueous and saltwater environments at relatively low temperatures, *i.e.*, at temperatures less than about 30°C. This has yielded a test method which gives a quantitative ranking order for the durability of adhesive systems and, furthermore, the results may be combined with a finite-element analysis of a bonded component or structure to give an estimate of its fatigue life in the environment of interest [4]. However, the cyclic-fatigue tests require expensive test equipment and are often time consuming to undertake, typically involving continued use of the fatigue test equipment for several months.

The main aim of the present work is to study the use of monotonically loaded tests as a method for assessing the joint durability. Fracture-mechanics tests have been conducted, using a tapered double-cantilever beam (TDCB) specimen, and the essence of the test procedure is the examination of the failure behaviour over a wide range of rates of displacement. In order to assess joint durability, tests have been carried out at various levels of relative humidity (RH). Further, two different substrates, an aluminium alloy and a steel, have been employed, along with either (1) a grit-blast and degrease (GBD) pretreatment or (2) a silane primer (GBS) pretreatment prior to bonding. The adhesive employed was a commercially available rubber-toughened epoxy. In addition, the loci of failure have been assessed using scanning electron microscopy (SEM) and X-ray photo-electron spectroscopy (XPS) to help identify the mechanisms of failure.

EXPERIMENTAL

Materials and Surface Pretreatments

To determine the adhesive fracture energy, G_c, an adhesively-bonded tapered double-cantilever beam (TDCB) specimen was employed (Figure 1). The adhesive employed was a hot-cured, rubber-toughened, epoxy-paste adhesive that was based upon a diglycidyl ether of bisphenol- A epoxy cured with dicyandiamide. The substrates were manufactured from either steel (Grade BS 970 070M55) or aluminium alloy (Grade BS 7075 (unclad)). Their compositions are given in Tables 1 and 2, respectively.

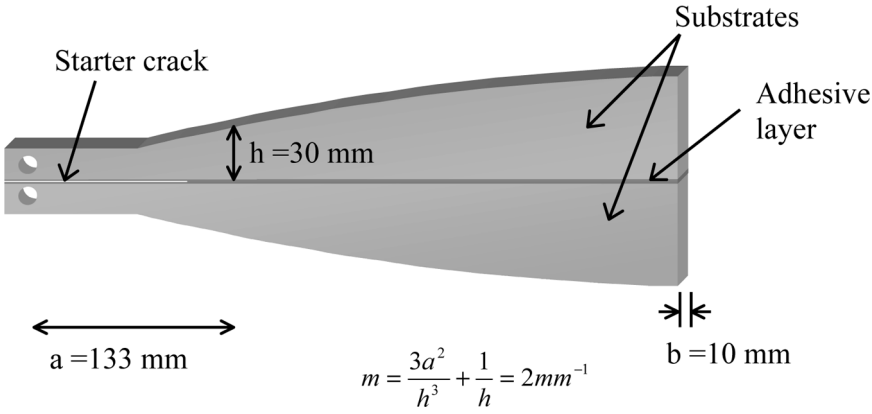

FIGURE 1 The tapered double-cantilever beam (TDCB) joint (dimensions are in mm).

TABLE 1 Chemical Composition of BS 970 070M55 Steel (by Weight)

C	Mn	Si	S	P	Fe
0.5–0.6%	0.5–0.8%	0.15–0.35%	0.04% max	0.04% max	balance

For both types of substrate, two different surface pretreatments prior to bonding were employed. The first surface pretreatment consisted of degreasing the substrates in a liquid bath of boiling 1,1,1-trichloroethylene, which was followed by grit-blasting using 60–78 μm mesh alumina particles. The substrates were then vapour degreased above a bath of boiling trichloroethylene and allowed to cool to room temperature. This pretreatment is denoted as the GBD pretreatment. In the second pretreatment employed, the previous grit-blasting and degreasing procedures were first undertaken and then followed by the application of a silane-based primer, to give the GBS pretreatment. A 1% w/w solution of γ-glycidoxypropyltrimethoxy silane solution, using a 90:10 by weight of ethanol:deionised water mixture, was prepared and its pH was adjusted to approximately five by the addition of acetic acid. This solution was stirred for 60 min. to allow complete hydrolysis of the GBS to occur. The solution was then painted onto the surfaces of the substrates that were to be bonded, using a small brush. The substrates were drained onto a tissue and the silane layer was cured at 93°C for 60 min. This procedure is very similar to that recommended by Digby and Shaw [5].

Joint Preparation

At the end of the substrates where the load was to be applied, a thin layer of silicon-based release agent was painted over a length of about 90 mm of the substrate surface to act as a precrack. Applying the release agent with a "chevron-shaped" end was found to give a precrack that tended to promote stable failure, as opposed to unstable failure, as described below.

The adhesive was degassed under vacuum for a short time at 80°C and was then applied to the faces of the substrates to be bonded using

TABLE 2 Chemical Composition of BS 7075 Aluminium Alloy (by Weight)

Zn	Mg	Cu	Cr	Fe	Si	Ti	Al
5.1–6.1%	2.1–2.8%	1.2–2.0%	0.18–0.4%	0.7% max	0.50% max	0.20% max	balance

a spatula. The thickness of the adhesive layer was 0.4 mm and was controlled *via* thin steel wires inserted into either end of the TDCB specimen. The adhesive layer was cured by heating the adhesive for 2 h at 130°C, as monitored *via* an *in situ* thermocouple, and the joints were then cooled in the oven overnight.

Fracture Mechanics Tests

Tests were conducted at a constant rate of displacement, $\dot{y}$, of the crosshead of the tensile testing machine and the crack length was monitored as a function of time using a video camera. The rate of displacement used for these monotonically loaded tests was varied between 0.005 to 10 mm/min. The tests were conducted at 21 ± 2°C in an environmental chamber, which permitted a wide range of RHs to be employed. The RH in the environmental chamber was controlled using various salt solutions [6] and was measured using a hair hygrometer. The experimentally measured RH values were in close agreement with the expected RH values (see Table 3).

The value of the adhesive fracture energy, G_c, was determined using the expression

$$G_c = \frac{P_c^2}{2b} \cdot \frac{dC}{da}, \tag{1}$$

where P_c is the critical load for crack growth as discussed below, a is the crack length, b is the width of the specimen, and C is the compliance of the specimen ($C = y/P$; where y is the displacement and P is the load).

TABLE 3 Expected and Measured Relative Humidities (RHs) Obtained from Using the Saturated Salt Solutions

Saturated salt solution	Expected RH (%)	Measured RH (%)
$CaHPO_4.2H_2O$	95	96–98
Na_2SO_4	93	88–94
$(NH_4)_2SO_4$	81	78
$NaNO_2$	66	58–72
KNO_2	45	48–50
$CaCl_2$	32	36–38
CH_3COOH	20	19–22
$ZnCl_2$	10	10–13
P_2O_5	0	1–5

Examination of the Fracture Surfaces

In the present work, a JEOL JSM 5300 scanning electron microscope (Jeol, Welwyn Garden City, UK) was used to examine the surfaces of the fractured joints. As it is not always possible to determine with certainty the locus of failure using a scanning electron microscope (for example, a very thin layer of adhesive or oxide would not be detectable), X-ray photoelectron spectroscopy was also employed. The apparatus used in the present study was a VG Scientific Sigma Probe spectrometer (VG, East Grinstead, UK). Survey spectra were acquired with a pass energy of 100 eV and the high resolution spectra with a pass energy of 50 eV. Quantitative surface chemical analyses and peak fitting were undertaken on the high resolution spectra using the software provided by the manufacturer.

CRACK PROPAGATION STUDIES AT 55% RH

Before considering the effects of the RH of the test environment on the bonded joints in detail, it is useful to consider the general form of the relationships which were obtained between the adhesive fracture energy, G_c, and the corresponding crack velocity, $\dot{a}$. These are shown in Figures 2 and 3 for the aluminium alloy and the steel joints that were tested at 55% RH (which was the ambient RH in the air-conditioned laboratory) where the data are plotted in the form of $\log_{10} G_c$ *versus* $\log_{10} \dot{a}$. In these figures, results for the two pretreatments (*i.e.,* the GBD and GBS) are given for both types of joints. Three different regions of crack growth behaviour may be identified. These have been labelled "Region I," "Region II," and "Region III," following the classic studies of Wiederhorn [7] on crack growth in glass. Region I occurred at relatively low rates of displacement, and the fracture was stable in nature and was visually interfacial, whereas Region III was observed at relatively high rates of displacement and the fracture was unstable and essentially cohesive in the adhesive layer. Region II was the transition region between Region I and Region III.

Region I Behaviour

This region was observed at relatively low rates of displacement, $\dot{y}$, and the crack propagated in a stable manner visually along the substrate/adhesive interface. During crack growth in Region I, the load was essentially constant at a value of P_c, and a typical load, P, *versus* displacement, y, curve associated with stable crack growth is shown in Figure 4. The average value of the load, P_c, for crack growth was

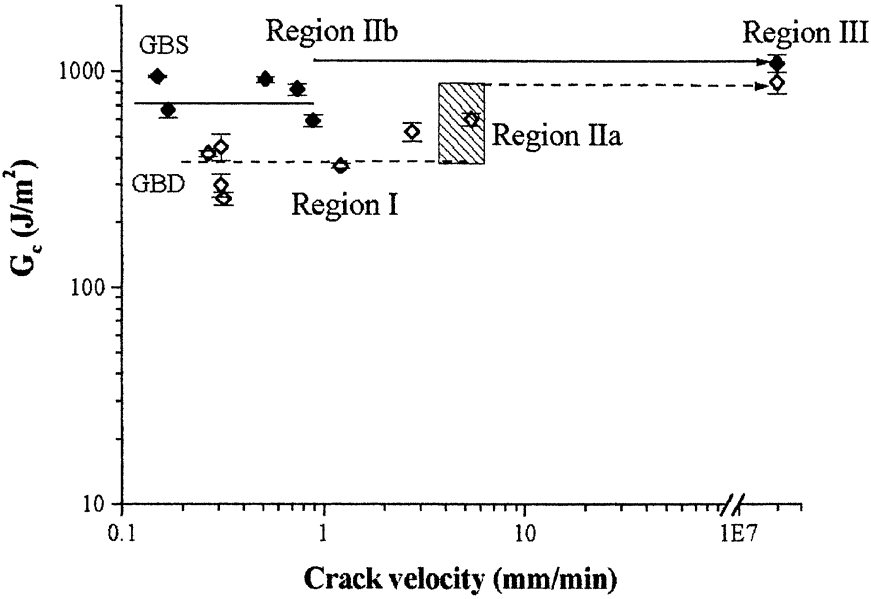

FIGURE 2 Relationship between the fracture energy, G_c, and the crack velocity, $\dot{a}$, for the GBD- and GBS-pretreated aluminium alloy joints. (The solid or dashed lines ending with an arrowhead indicate that no results could be obtained in this range, since the type of crack growth changed from stable to unstable, as discussed in the text; filled points, GBS pretreated; open points, GBD pretreated.)

employed to determine the value of the adhesive fracture energy, G_c, as indicated above (see Equation (1)).

For a test at a given rate of displacement, $\dot{y}$, the relationship between crack length, a, and time, t, was linear (as shown in Figure 5), which leads, of course, to a constant value of the crack velocity, $\dot{a}$, throughout the test as the crack propagates down the length of the TDCB specimen. The higher the rate of displacement employed within Region I, the higher the resulting crack velocity, as illustrated in Figure 6. Thus, for a given joint system, the crack velocity, $\dot{a}$, is controlled by the rate of displacement, $\dot{y}$, of the crosshead. A theoretical relationship between $\dot{a}$ and $\dot{y}$ may be derived using simple beam theory [8], assuming that the load, P_c, at fracture remains constant for a given TDCB test. Thus, the derivative of the compliance is given by

$$\dot{C} = \frac{1}{P_c} \cdot \dot{y}. \tag{2}$$

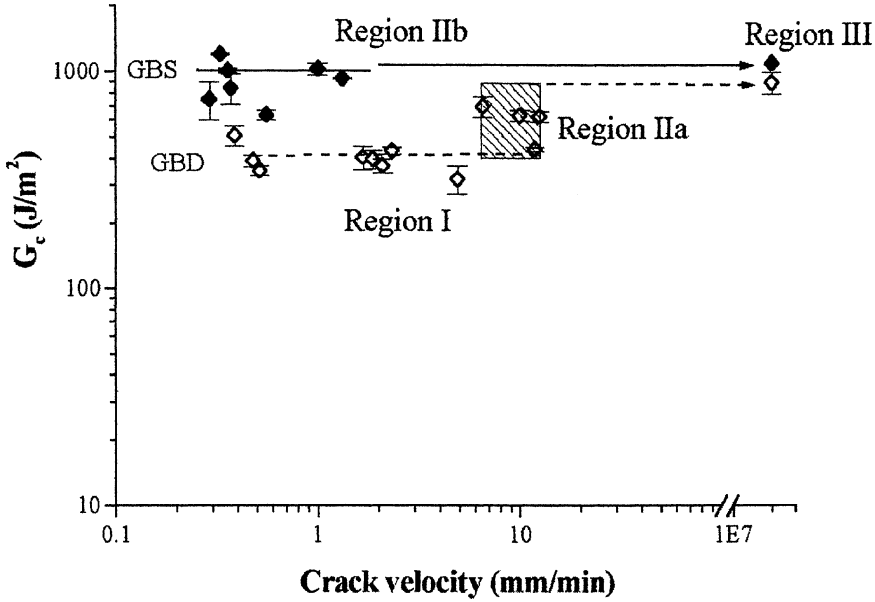

FIGURE 3 Relationship between the fracture energy, G_c, and the crack velocity, $\dot{a}$, for the GBD- and GBS-pretreated steel joints. (The solid or dashed lines ending with an arrowhead indicate that no results could be obtained in this range, since the type of crack growth changed from stable to unstable, as discussed in the text; filled points, GBS pretreated; open points, GBD pretreated.)

Rearranging Equation (1) using Equation (2) yields

$$\dot{a} = \frac{P_c}{2bG_c} \cdot \dot{y}. \tag{3}$$

The values of the crack velocity, $\dot{a}$, *versus* the applied rate of displacement, $\dot{y}$, of the crosshead from both the experiments and Equation (3) are shown in Figures 6a and 6b for the aluminium alloy and the steel joints, respectively. The agreement between the experimental and the theoretical values is relatively good.

As may be seen from Figures 2 and 3 for the aluminium alloy and steel joints, respectively, in Region I the value of G_c is not greatly dependent upon the value of the corresponding crack velocity, $\dot{a}$. The locus of joint failure associated with this type of stable crack growth in Region I was always visually interfacial between the adhesive and the substrate. In Figures 2 and 3, the final point shown for the G_c *versus* $\dot{a}$ relationships (*i.e.*, at the highest value of $\dot{a}$) for Region I

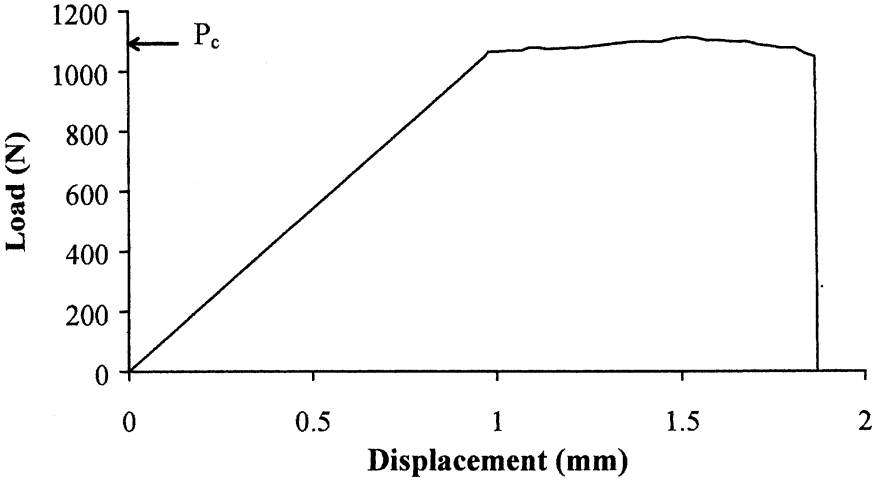

FIGURE 4 Typical load, P, *versus* displacement, y, curve associated with stable crack growth, as seen in Region I (and Region II). The specimen was a GBD-steel joint tested at 0.1 mm/min at 55% RH.

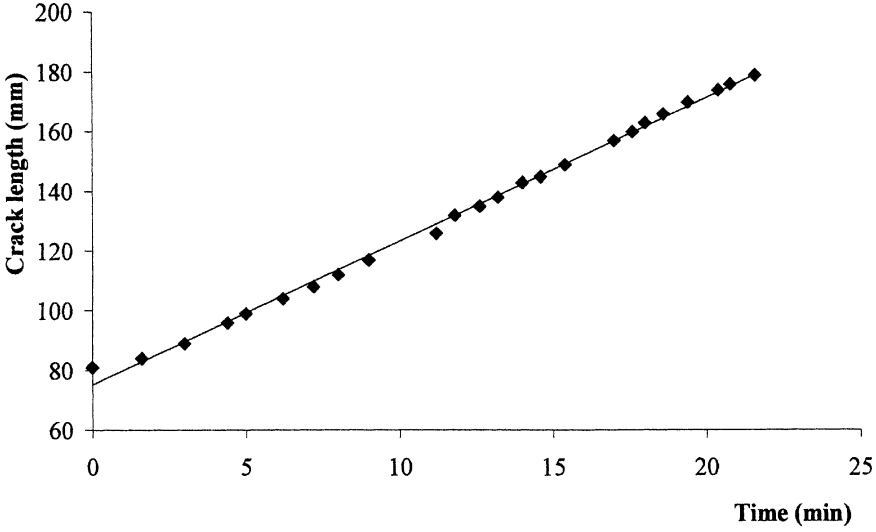

FIGURE 5 Relationship between crack length, a, and time, t, as seen in Region I. The specimen was a GBD-steel joint tested at 0.05 mm/min at 55% RH.

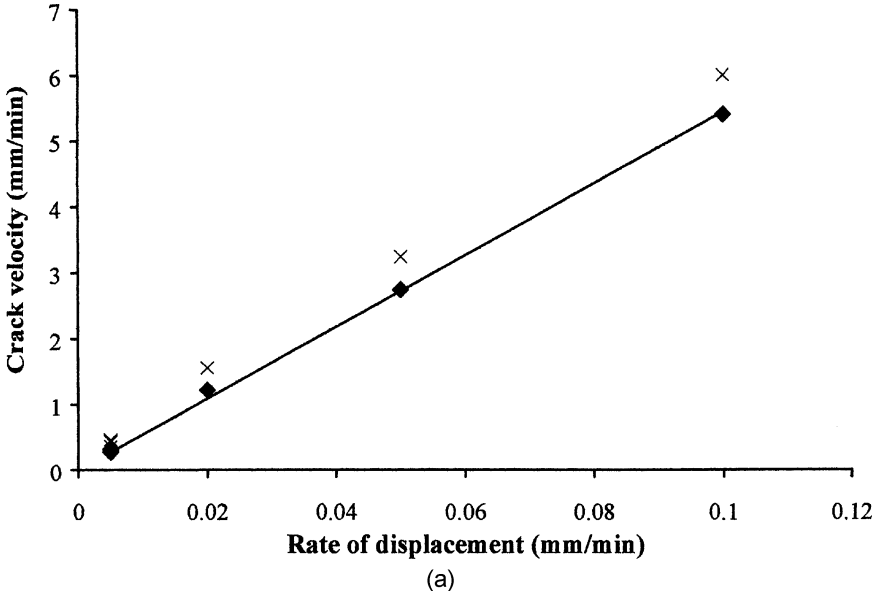

FIGURE 6 Relationship between crack velocity, $\dot{a}$, and rate of displacement, $\dot{y}$, as seen in Region I for (a) the aluminium alloy joints and (b) the steel joints. For each type of substrate: ◆,experimental points; x, points given by Equation (3). The straight line plotted represents the best statistical fit for the experimental data, as obtained *via* a linear regression analysis. (Continued).

behaviour represents the fastest crack velocity that could be recorded. Indeed, increasing the rate of displacement of the test above this value by a small increment led to the observation of Region II or Region III behaviour.

Region III Behaviour

Region III behaviour was observed at relatively high rates of displacement, $\dot{y}$. Here the crack grew in an unstable, stick-slip manner with the crack growing in an uncontrolled way, at a relatively fast velocity, and then arresting. These observations are clearly in direct contrast to the results from Region I. Furthermore, unlike that found in Region I, the locus of joint failure in Region III was always essentially cohesive through the adhesive layer.

This type of unstable crack growth has a significant effect on the associated load, P, *versus* displacement, y, curve which now had a characteristic saw-tooth appearance, as may be seen from Figure 7.

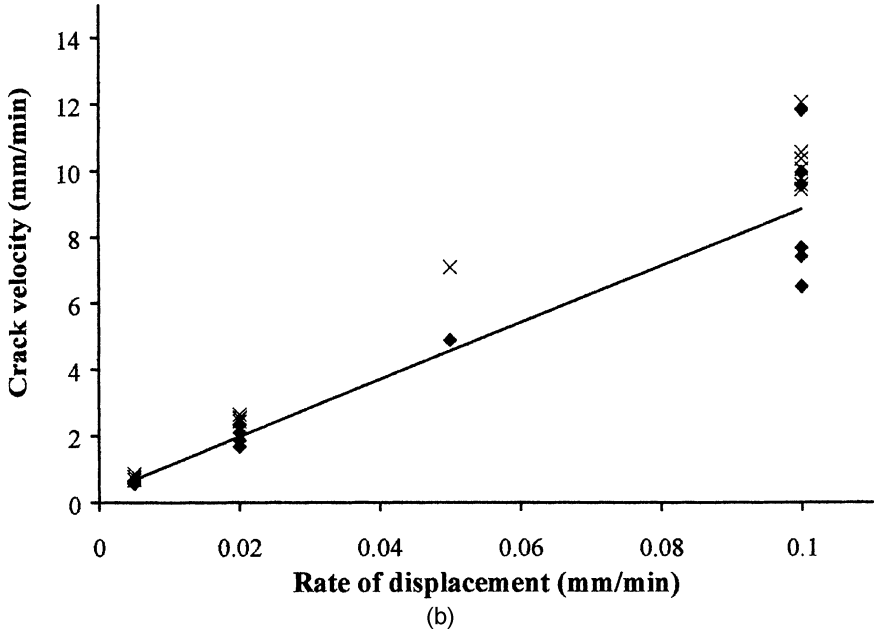

FIGURE 6 (Continued.)

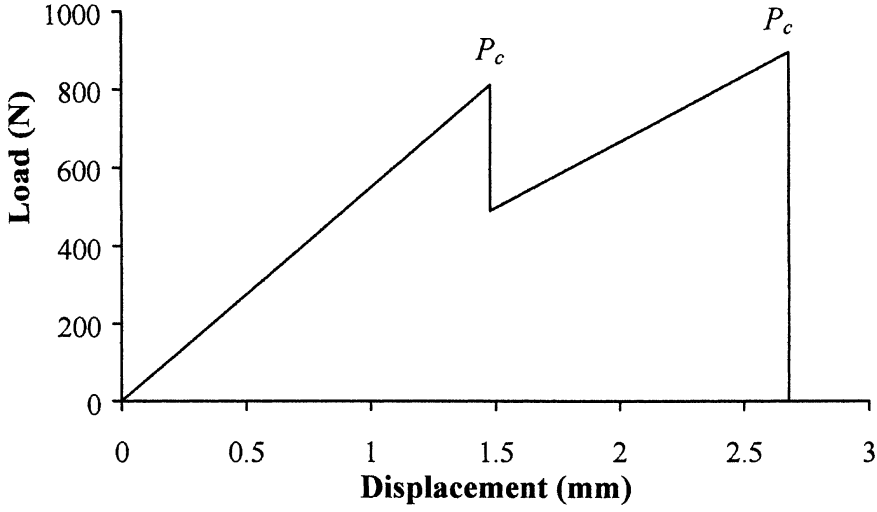

FIGURE 7 Typical load, P, *versus* displacement, y, curve associated with stick-slip crack growth, as seen in Region III. The peaks correspond to crack initiation and the valleys to crack arrest. The specimen was a GBS -pretreated aluminium alloy joint tested at 0.1 mm/min at 55% RH.

The peak values of the load, P_c, represent the value of the load for the onset of crack growth, and the average of these values was used to determine the value of the adhesive fracture energy, G_c, as indicated above. The values of G_c obtained are of the order expected for this type of adhesive [4]. When unstable crack growth was observed the crack propagated at a relatively high velocity, which was too high to be measured using the video camera. However, an approximate value of the crack velocity was estimated from previously published data by Gledhill and Kinloch [9]. They applied a grid of conductive paint to the side of the TDCB specimen and, *via* the change in electrical resistance of the grid as the crack propagated and ruptured the paint grid, obtained the relationship between G_c and $\dot{a}$ for a similar adhesive system that exhibited unstable crack growth. Using the data of Gledhill and Kinloch [9], the crack velocity corresponding to the G_c value in Region III for the present tests was about 20 km/min for both the GBD-and GBS-pretreated joints. This value was, therefore, taken to represent the resulting crack velocity for unstable crack growth in the present studies. This is obviously an approximation, but the absolute value of the crack velocity associated with the unstable crack growth Region III has no significant effect on the interpretation of the results obtained in the present study.

Finally, it is noteworthy that Arnott and Kindermann [10] have also studied the effect of a constant rate of displacement on the value of G_c of structural joints. Although they did observe in their experiments what we have termed Region III behaviour, such cohesive failure in the adhesive layer was still associated with stable crack growth.

Region II Behaviour

Region II is a transition region between Region I and Region III. Two subtypes of Region II were identified as explained below, denoted as Region IIa and Region IIb, respectively.

In the transition region Region IIa data could be obtained for joints where the values of G_c were intermediate between those recorded in Region I and those in Region III. This behaviour may be seen clearly in Figures 2 and 3 for the GBD-pretreated aluminium alloy and steel joints, respectively. In Region IIa, the locus of joint failure associated with this type of stable crack growth was always visually interfacial between the adhesive and the substrate, as was observed in Region I.

In Region IIb it was not possible to obtain experimental data in the transition region between Region I and Region III, as it was for Region IIa. Furthermore, in some instances the increase in the value of G_c ongoing from Region I to Region III behaviour was relatively low.

The regions denoted Region IIb in Figures 2 and 3 for the GBS-pretreated aluminium alloy and steel joints, respectively, illustrate both of these aspects for the Region IIb behaviour. Thus, the term Region IIb is simply used to represent a change in the type of crack growth, *i.e.*, from stable to stick-slip crack growth, which is always accompanied by a change from visually interfacial to visually cohesive failure in the adhesive as the rate of displacement, $\dot{y}$, is steadily increased.

Effect of Substrate

As noted above, the results for the values of G_c as a function of corresponding crack velocity, $\dot{a}$, are shown for the aluminium alloy and steel joints in Figures 2 and 3, respectively. For the data associated with both Region I and Region III, there is no statistical difference in the values of G_c associated with the aluminium-alloy and steel joints for a given type of surface pretreatment.

Effect of Surface Pretreatment

The effect of the type of surface pretreatment employed is evident in all three regions of the fracture behaviour of these joints, as may been seen from Figures 2 and 3.

In Region I, the values of G_c for the GBS-pretreated joints are clearly higher than for the GBD-pretreated joints for both the aluminium alloy and the steel substrates, although the locus of failure was visually at, or very close to, the adhesive/substrate interface for all these types of joint. Nevertheless, it is noteworthy that the slope of the G_c *versus* $\dot{a}$ relationship is not affected by the surface pretreatment employed.

In Region III, the values of G_c for the GBS-pretreated joints were again somewhat higher than for the GBD-pretreated joints, and this was observed for both the aluminium alloy and the steel joints, even though the locus of failure was essentially cohesive in the adhesive layer in all cases. The values of G_c, considering both types of substrate, were 1010 J/m^2 ($\pm$ 100 J/m^2) and 780 J/m^2 ($\pm$ 100 J/m^2) for the GBS- and GBD-pretreated joints, respectively. This intriguing observation is discussed in more detail below when the mechanisms of failure are examined.

Finally, considering the onset of Region II behaviour, the maximum velocity that could be sustained in Region I, before the transition to Region III behaviour was observed, was far greater for the GBD-pretreated joints than for the GBS-pretreated joints. For instance,

the maximum velocity measured in Region I for the GBD-pretreated aluminium alloy joints was 5 mm/min, whereas for the GBS-pretreated aluminium alloy joints it was 1 mm/min. Thus, the transition Region II occurred in the GBD-pretreated joints at a significantly higher rate of displacement than in the GBS-pretreated joints.

EFFECT OF RH

To explore the interactions between the RH and the rate of displacement, first the relationships shown above between the adhesive fracture energy, G_c, and the corresponding crack velocity, $\dot{a}$, at 55% RH were studied for the GBD-pretreated aluminium alloy joints as a function of the RH. These results are shown in Figure 8.

In Region I, the slopes of the G_c *versus* $\dot{a}$ relationships obtained at the different values of RH are essentially the same, although the height of the G_c *versus* $\dot{a}$ relationship, with respect to the G_c axis, is very dependent upon the value of the RH employed, for example,

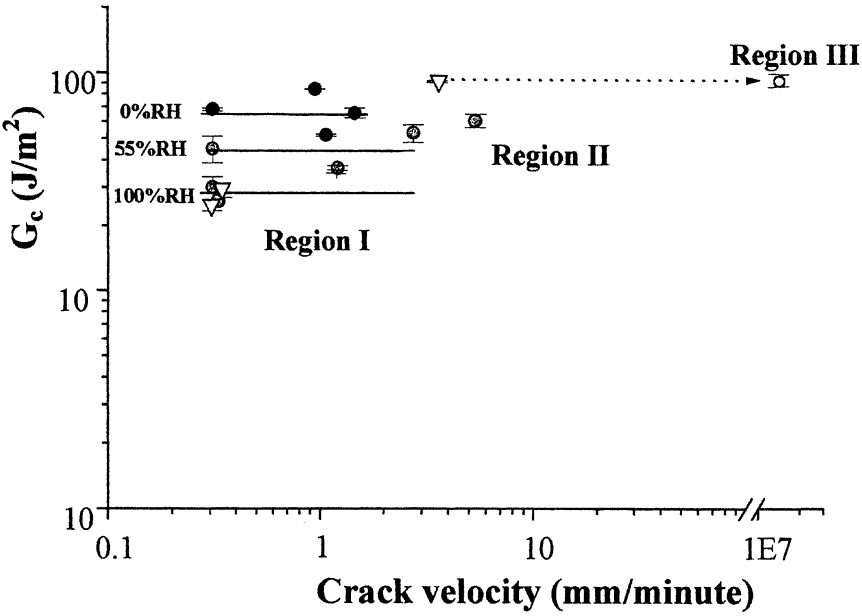

FIGURE 8 Relationship between the fracture energy, G_c, and the crack velocity, $\dot{a}$, for the GBD-pretreated aluminium alloy joints obtained at 0%, 55%, and 100% RH. Filled circles, 0% RH; open circles, 55% RH; open diamonds, 100% RH.

$G_c \approx 700$ J/m^2 at 0% RH but $G_c \approx$ 300J/m^2 at 100% RH. It is very noteworthy that there is Region I behaviour observed at 0% RH, and it is considered that the use of P_2O_5 would indeed give a 0% RH test environment (see Table 3). This demonstrates that Region I behaviour is not solely the result of the presence of water molecules at the crack tip. This observation from the present work is discussed further below.

Considering Region III, it may be seen that there is no significant effect of the relative humidity on the value of G_c in this region where unstable, stick-slip crack growth is observed. Indeed, since the locus of failure is cohesive in the adhesive and the timescale of the experiment gives relatively little scope for water diffusion and plasticisation of the adhesive, this observation would indeed be expected.

Effect of RH and Surface Pretreatment in Region I

From the above results, it is evident that the most pronounced effects of varying the RH are seen in Region I, when the crack velocity is relatively low and the joints exhibit a visual locus of failure at the adhesive/substrate interface. The effect of RH was, therefore, explored in detail by selecting a rate of displacement which should essentially lead to Region I behaviour, although some Region III behaviour was still recorded at the lowest RHs, as will be seen below. The GBD-
pretreated aluminium alloy joints were, therefore, tested at a rate of displacement of 0.02 mm/min, while the GBS-pretreated aluminium alloy joints were tested at a rate of displacement of 0.005 mm/min. The resulting average crack velocities were 1.15 ± 0.20 mm/min and 0.25 ± 0.10 mm/min for the GBD- and GBS-pretreated joints, respectively.

The GBD-Pretreated Aluminium-Alloy Joints

The results for the GBD-pretreated aluminium-alloy joints tested at a rate of 0.02 mm/min are shown in Figure 9, where the value of G_c is given as a function of the measured RH. The straight line plotted through these data represents the best statistical fit *via* a linear regression analysis to the results which exhibited stable crack growth, *i.e.*, Region I behaviour. As may be seen, the vast majority of the joints tested exhibit Region I behaviour, and there is a clear dependence of the value of G_c upon the RH, with the value of G_c decreasing steadily as the RH is increased. However, at the lowest values of RH, a few joints exhibited Region III behaviour and thus failed cohesively through the adhesive layer with a relatively high value of G_c being recorded.

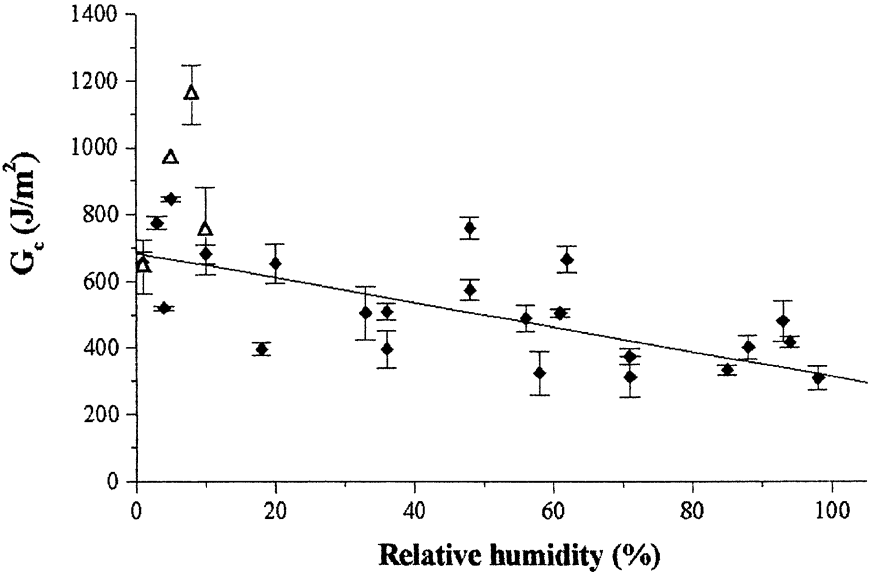

FIGURE 9 Relationship between the fracture energy, G_c, and crack velocity, $\dot{a}$, as a function of the RH for the GBD-pretreated aluminium alloy joints: Δ, joints exhibiting stick-slip crack growth; ◆, joints exhibiting stable crack growth.

The GBS-Pretreated Aluminium Alloy Joints

The results for the GBS-pretreated aluminium alloy joints tested at a rate of 0.005 mm/min are shown in Figure 10, where the value of G_c is given as a function of the measured RH. Again, the straight line plotted through these data represents the best statistical fit *via* a linear regression analysis to the results which exhibited Region I behaviour. As observed for the GBD-pretreated joints, the vast majority of the joints tested exhibited Region I behaviour, and the value of G_c decreases steadily as the RH is increased. However, at the lowest values of RH, the joints consistently exhibited Region III behaviour and thus failed cohesively through the adhesive layer with a relatively high value of G_c being recorded.

There are some noticeable differences arising from the effects of the two different surface pretreatments. Firstly, at relatively low values of RH, the transition from Region III to Region I behaviour is far more marked for the GBS-pretreated joints than for the GBD-pretreated joints. Indeed, for the GBS-pretreated joints one could infer that a critical RH of about 20% RH exists, below which interfacial attack

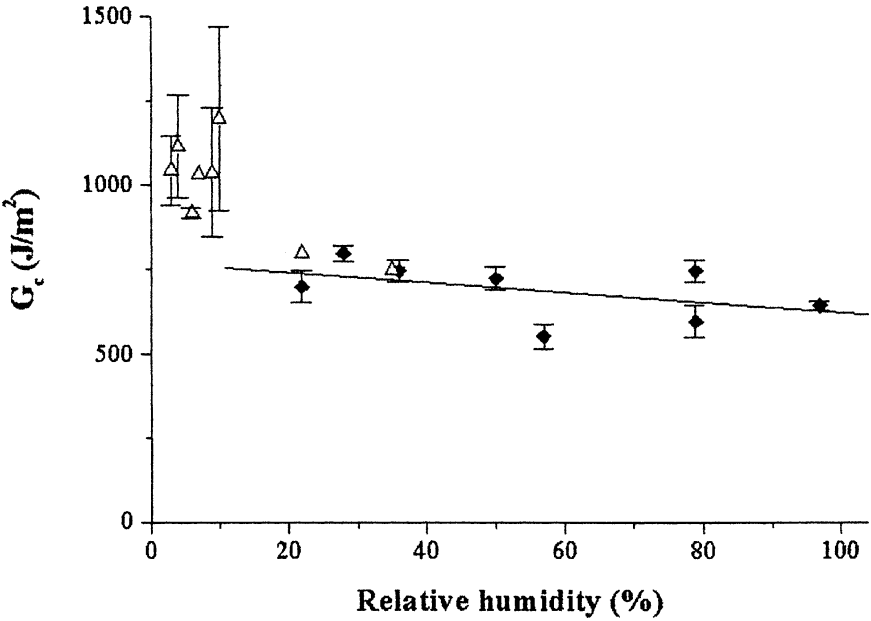

FIGURE 10 Relationship between the fracture energy, G_c, and the RH for the GBS-pretreated aluminium alloy joints: (Δ, joints exhibiting stick-slip crack growth; ◆, joints exhibiting stable crack growth.

and weakening of the joints does not occur. The concept that a minimum, or critical, concentration of water needs to be present in order for the mechanism of environmental attack to proceed has been previously suggested (*e.g.*, Gledhill *et al.* [11] and Brewis *et al.* [12]) and obviously is in agreement with the transition currently observed between the Region I and the Region III behaviour, as discussed in detail below. Secondly, for the GBS-pretreated joints the levels of G_c are significantly higher for both Region I and Region III behaviour. This may be readily seen from Figure 11, where the data from Figures 9 and 10 are directly compared. The underlying mechanisms for this observation are discussed below. (Note that in Figure 11 the slope for the results of G_c *versus* RH for the GBD-pretreated joints (see Figure 9) is replotted to have the same slope as for the GBS-pretreated joints (see Figure 10), since this is within the experimental scatter band.)

MECHANISMS OF FAILURE IN REGION I

The above results have led to several interesting observations, and they highlight the interaction between the rate of displacement, the

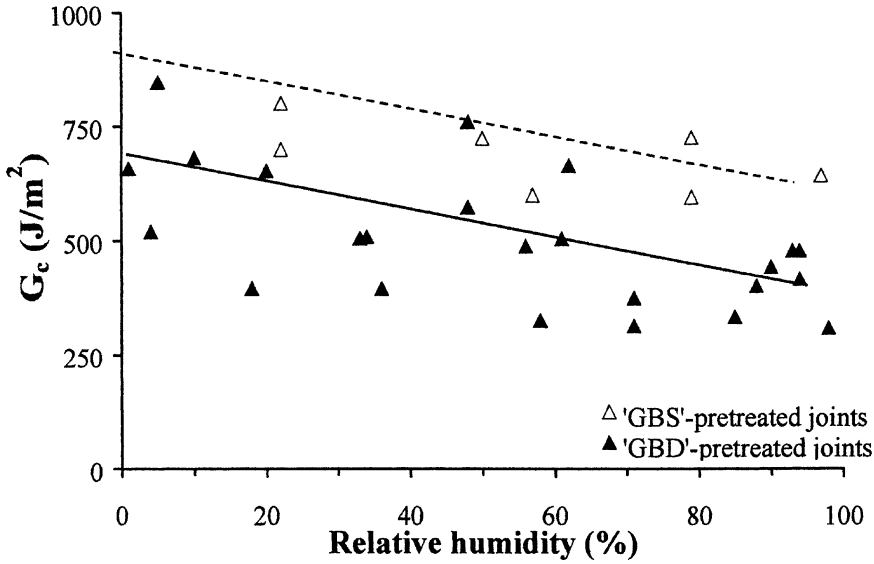

FIGURE 11 Comparison of the relationships between the fracture energy, G_c, and the RH obtained for the GBD-pretreated aluminium alloy joints and the GBS-pretreated aluminium alloy joints for the stable crack growth regime, Region I.

RH of the test environment, and the type of surface pretreatment employed. The mechanisms of failure responsible for these observations will now be considered.

The Relationship Between G_c and $\dot{a}$

From the results shown in Figures 2, 3, and 8 the relationship between G_c *versus* $\dot{a}$ may be described by a power-law equation of the form

$$G_c \propto \dot{a}^n, \tag{4}$$

where the slope of the relationship is given by the power, n. Furthermore, n clearly is relatively low in value and is independent of the RH, the type of substrate, and the surface pretreatment employed.

Previous workers [13–15] have found a similar relationship for crack growth in thermoplastic and thermosetting polymers that is also associated with a relatively low value of n. Williams [14] has postulated that viscoelastic processes occurring at the crack tip control the dependence of G_c upon the crack velocity, $\dot{a}$, and that the value of n is related to the polymer's viscoelastic properties by

$$tan\frac{\pi n}{2} = \tan\delta_r, \tag{5}$$

where $\tan\delta_r$ is the viscoelastic loss factor. For the epoxy adhesive, from dynamic mechanical thermal analysis (DMTA) studies, the value of $\tan\delta_r$ at room temperature and a relatively low test frequency of 1 rad/s is 0.014 [16]. From Equation (5), this value of $\tan\delta_r$ yields a value of $n \approx 0.01$. This value of $n \approx 0.01$ would obviously give an excellent fit to the slopes of the G_c *versus* $\dot{a}$ relationships shown in Figures 2, 3, and 8, *i.e.*, very little rate dependence of the value of G_c is observed in Region I. Also, this value of n is in very good agreement with values from previous work where the bulk fracture of epoxy polymers was studied [9].

Thus, from (1) the current values of n being very similar as deduced from the fracture tests and the DMTA studies and (2) by analogy to previous work [13–15], it appears that the viscoelastic processes which operate in the vicinity of the crack tip control the rate dependence of the toughness, G_c, of the present adhesive joints. This explains why no effect of the RH, substrate type, or surface pretreatment used is observed with respect to the rate dependence; *i.e.,* with respect to the slope, n, of the G_c *versus* $\dot{a}$ logarithmic relationship.

Constant Crack Opening Displacement Criterion

When the rate dependence of the G_c *versus* $\dot{a}$ relationship is governed by viscoelastic processes that occur in the viscoelastic plastic zone ahead of the crack tip, then it is invariably found that the fracture process can be considered to be controlled by a critical value of the crack opening displacement, δ_t, where the value of δ_r is given by

$$\delta_t = \frac{G_c}{\sigma_y}, \tag{6}$$

and where σ_y is the uniaxial yield stress of the polymer or polymeric adhesive layer.

The yield stress of the adhesive used in the present studies was measured *via* plane-strain compression tests and was found to increase somewhat as the strain rate, $\dot{\varepsilon}$, was increased, as would be expected: the uniaxial yield stress, σ_y, so deduced increased from 71 MPa to 75 MPa as the strain rate was increased over two decades.

From Equation (7), the value of the critical crack opening displacement, δ_t, may be deduced, and since there is very little rate dependence of the terms G_c or σ_y a constant value of δ_t, independent of

crack velocity, is obtained. For the GBD- and the GBS-pretreated joints, the values of the critical crack opening displacement were calculated to be about 5 μm and 12 μm, respectively. These values are not significantly dependent upon the type of substrate, but the far higher value of δ_t ascertained for the GBS-pretreated joints again reflects the superior durability offered by this form of surface pretreatment.

Environmental Attack

First, it must be underlined that interfacial fracture in Region I is not intrinsically the result of environmental attack, since joints tested at 0% RH were observed to exhibit Region I behaviour and hence to fail visually along the interface between the adhesive and the substrate. However, there is a clear effect of the RH of the test environment in Region I: the higher the RH, the lower the adhesive fracture energy (see Figures 8 to 11). As commented above, the type of substrate (*i.e.*, whether aluminium alloy or steel) appears to play no significant role in the degree of environmental attack, but the choice of surface pretreatment (*i.e.*, GBD *versus* GBS) and the concentration of water (*i.e.,* the RH) are critical factors, as may be seen from Figures 9 to 11. Nonetheless, it should again be emphasised that, while the absolute value of G_c is a function of these parameters, the dependence of G_c upon the crack velocity, $\dot{a}$, is controlled by the viscoelastic nature of the epoxy adhesive, as discussed above.

These observations firstly imply that in Region I, at values of RH greater than 0% RH, as the RH increases higher concentrations of water reach the vicinity of the crack tip and increasingly attack and weaken the interphase regions of the joints. Hence, the value of G_c decreases, although a critical concentration of water molecules may have to be attained in the case of the GBS-pretreated joints before any environmental attack mechanism may be initiated. Secondly, the water molecules reach the vicinity of the crack tip at a sufficiently fast rate to enable the environmental attack mechanism to occur readily, since the G_c *versus* crack velocity dependence is controlled by the viscoelastic nature of the epoxy adhesive, not by the RH employed.

The GBD-Pretreated Joints

In the case of the GBD-pretreated joints, the intrinsic stability of the adhesive/substrate interface in the presence of an aqueous environment in the long term may be assessed from the thermodynamic arguments advanced by Gledhill and Kinloch [17]. The thermodynamic work of adhesion is defined as the energy required to separate

unit area of two phases forming an interface. If only secondary forces (*e.g.*, van der Waals forces) are acting across the interface which is considered to be the main mechanism of adhesion of most epoxy adhesives, then the work of adhesion, W_A, in an inert medium may be expressed by

$$\overline{W}_A = \gamma_a + \gamma_s - \gamma_{as}, \tag{7}$$

where γ_a and γ_s are the surface free energies of the adhesive and substrate, respectively, and γ_{as} is the interfacial free energy. In the presence of a liquid (denoted by the subscript l), such as water this expression must be modified, and the work of adhesion W_{Al} is now given by

$$W_{Al} = \gamma_{al} + \gamma_{sl} - \gamma_{as}, \tag{8}$$

where γ_{al} and γ_{sl} are the interfacial free energies between the adhesive/liquid and substrate/liquid interfaces, respectively. For an adhesive/substrate interface the work of adhesion, W_A, in an inert atmosphere (for example, dry air) usually has a positive value, indicating thermodynamic stability of the interface. However, in the presence of a liquid the thermodynamic work of adhesion, W_{Al}, may well have a negative value, indicating that the interface is now unstable and may dissociate. Thus, calculation of the terms W_A and W_{Al} may enable the long-term durability of the interface to be predicted. The values of W_A and W_{Al} for epoxy/steel joints, respectively, have been reported to be $+291$ and $-255\,\mathrm{mJ/m^2}$ [17]; and for epoxy/aluminium-alloy joints, $+232$ and $-137\,\mathrm{mJ/m^2}$ [18]. These values lead to the conclusion that the epoxy/oxide interfaces will indeed be susceptible to attack and degradation upon exposure to water molecules.

To assist in establishing the mechanisms of failure for the GBD-pretreated joint, the exact locus of failure in Region I was determined using SEM and XPS. The joints failed visually along the adhesive/substrate interface. Notwithstanding this observation, failure could have occurred within the adhesive layer, or oxide layer, with a very thin layer of adhesive, or oxide, retained on the opposite side of the joint which would be invisible to the naked eye. The substrate beam of a failed joint that visually appeared to have no adhesive left on its surface was referred to as the "metal" side, while the beam that was visually covered with adhesive was termed the "adhesive" side.

When the metal sides of a fractured GBD-pretreated aluminium alloy joint and a GBD-pretreated steel joint were examined using SEM, only a few isolated areas of the metal side of the joint appeared to be covered by any retained adhesive. The remainder of the surface

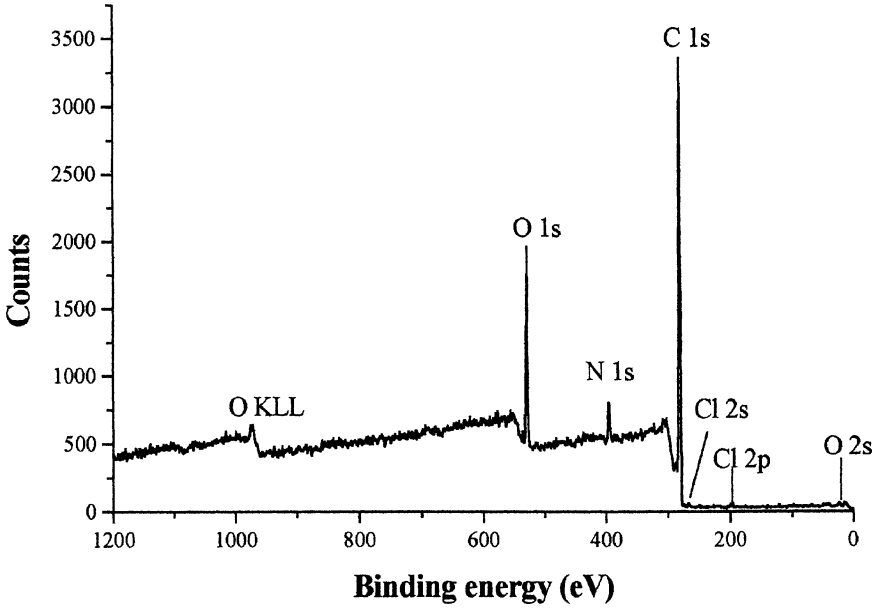

FIGURE 12 XPS spectrum of the cured adhesive.

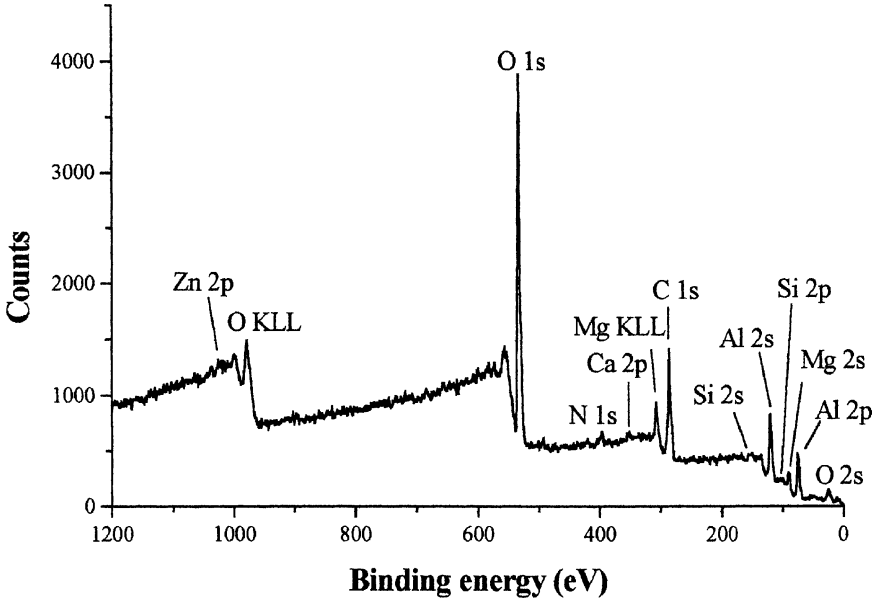

FIGURE 13 XPS spectrum of the GBD-pretreated aluminium alloy surface.

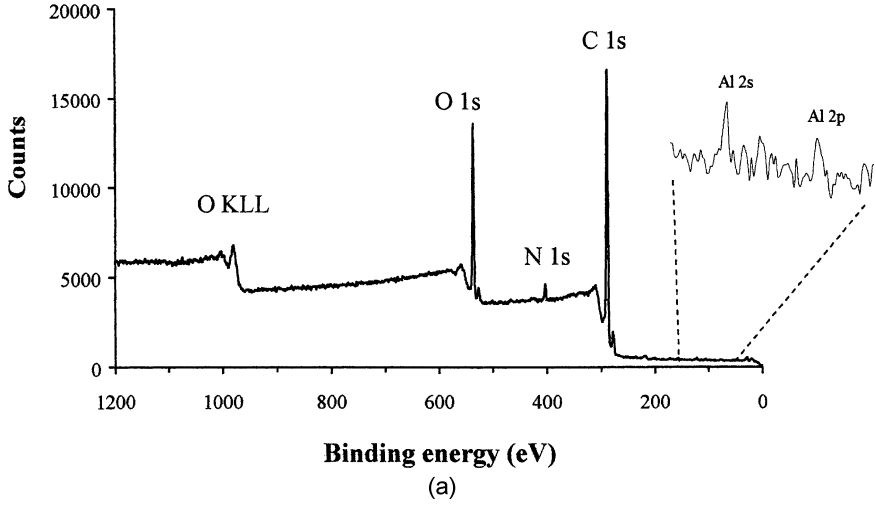

FIGURE 14 XPS spectra of a failed GBD-pretreated aluminium alloy joint: (a) adhesive side and (b) metal side (tested at 55% RH at a crack velocity of approximately 0.3 mm/min). (Continued).

appeared to be metallic in nature, implying that interfacial failure had occurred.

The XPS spectra of the control (*i.e.*, unbonded) adhesive and GBD-pretreated aluminium alloy materials are shown in Figures 12 and 13, respectively. As expected, the aluminium alloy surface prior to bonding is covered by a thin layer of carbonaceous contamination adsorbed from the atmosphere, as may be seen from the relatively strong C1s peak in Figure 13. However, previous work [19] has established that such contamination is readily absorbed and displaced during the bonding operation.

The XPS spectra of the adhesive and metal sides taken from a failed GBD-pretreated aluminium alloy joint, tested at 55% RH at a crack velocity of approximately 0.3 mm/min, are shown in Figures 14a and 14b, respectively. The spectrum of the adhesive side is rather similar to that of the control adhesive material (see Figure 12) and that of the metal side is very similar to that of the control GBD-pretreated aluminium alloy material (see Figure 13). This suggests that the failure occurred mainly along the adhesive/substrate interface. However, the presence of aluminium peaks in the spectrum of the adhesive side (see Figure 14a) reveals that the fracture occurred also to a small extent in the oxide layer. Further, the increase in the 'C/O' ratio in the XPS spectrum of the metal failure side (see Figure 14b) compared with

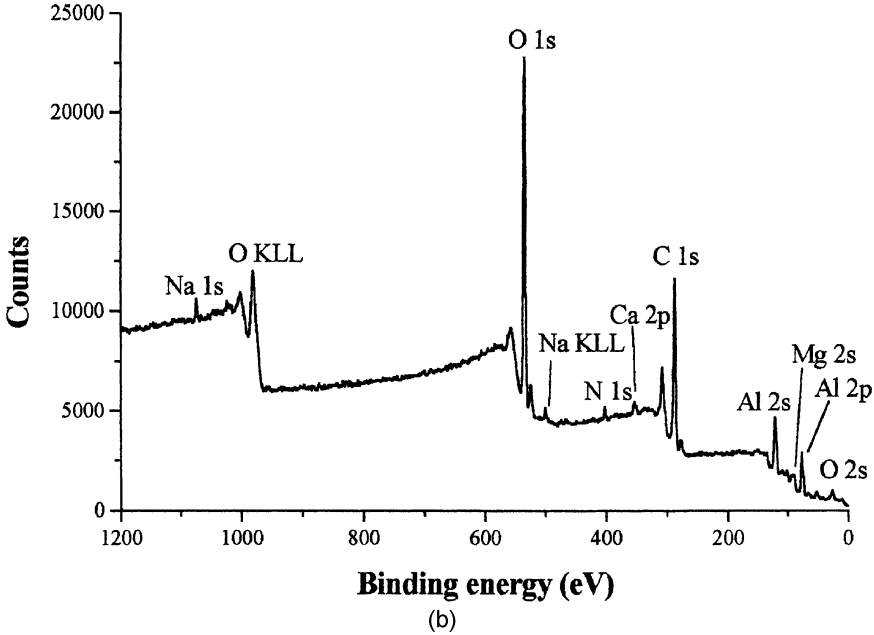

FIGURE 14 (Continued.)

that recorded from the control GBD-pretreated aluminium alloy (see Figure 13) is indicative of a small amount of adhesive being retained on the metal side. This observation is supported by the presence of a small N1s signal (at a binding energy of about 400 eV), which is presumably attributable to a curing agent or other, minor, component of the adhesive formulation. Thus, it may be concluded that the GBD-pretreated aluminium alloy joints failed mainly along the adhesive/substrate interface. However, the crack occasionally travelled in the oxide and in the adhesive layer, and this might simply be due to the crack growing through the oxide asperities and leaving adhesive retained in the "valleys" of the very rough surface as the crack travelled mainly along the substrate/adhesive interface. Similar conclusions were reached for the GBD-pretreated steel joints.

The fact that the fracture occurred mainly at the interface is in agreement with the thermodynamic arguments reported above. However, it should be borne in mind that the thermodynamic approach describes the behaviour of the joints at equilibrium (*i.e.*, over a relatively long time scale), and given the short length of the test (*i.e.*, a few hours) it is unlikely that the failure occurred solely as a result

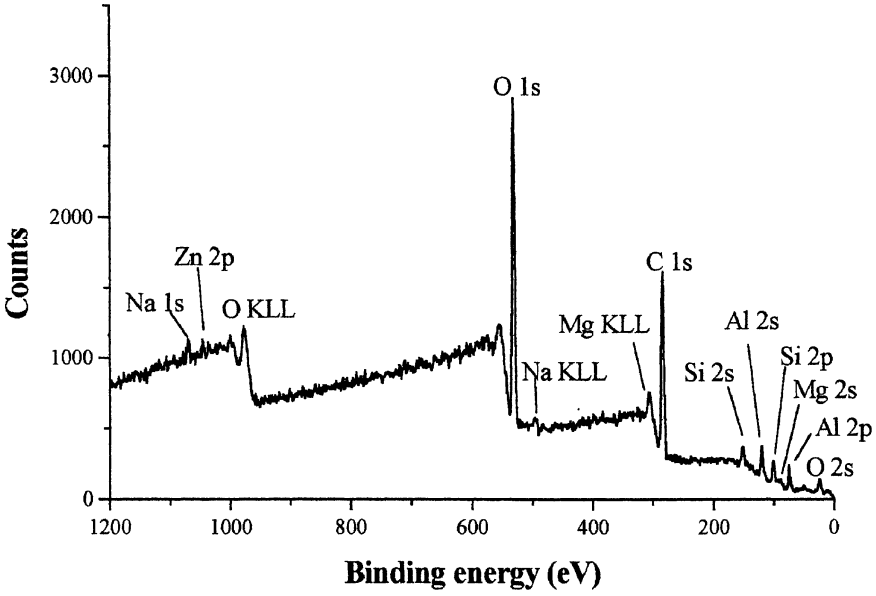

FIGURE 15 XPS spectrum of a GBS-pretreated aluminium alloy surface.

of the presence of water molecules. Thus, it is suggested that the joints failed due to both the application of a stress and the presence of water molecules at the crack tip, a phenomenon similar to stress corrosion cracking, which occurs in metals and ceramics (see, for example, Yahalom and Aladjem [20]). As the RH was increased, the number of water molecules was higher and the value of the adhesive fracture energy was seen to decrease, as indeed would be expected.

GBS-Pretreated Joints

Silane pretreatments are known to increase the degree of interfacial adhesion (see, for example, Gettings and Kinloch [21], Plueddeman [22], Davis and Watts [23], and Abel *et al.* [24]). This increase in the intrinsic adhesion has been attributed to the formation of covalent bonds between the metallic substrate and silane primer and, in turn, between the silane primer and the adhesive layer; *i.e.*, the silane primer acts as a "coupling agent." Indeed, covalent bonds between the substrates and the silane, based upon GPS, have been detected for steel [21, 23] and aluminium [24] using secondary ion mass spectrometry.

From using SEM, the metal side of a GBS-pretreated aluminium alloy joint and a GBS-pretreated steel joint appeared to be predominantly covered with adhesive.

The XPS spectra of the control (*i.e.*, unbonded) adhesive and GBS-pretreated aluminium alloy materials are shown in Figures 12 and 15, respectively. The XPS spectra of the adhesive and metal sides taken from a failed GBS-pretreated aluminium alloy joint, tested at 55% RH at a crack velocity of approximately 0.15mm/min, are shown in Figures 16a and 16b, respectively. The ratio of the C1s and O1s peaks in these spectra appear to be of the same order as that for the control adhesive (see Figure 12), which suggests that the failure occurred mainly in the adhesive layer. However, the presence of aluminium and silicon on the adhesive side of the GBS-pretreated aluminium alloy joint (see Figure 16a) suggests that fracture also occurred to a certain extent in the silane and oxide layers. This is presumably due to the asperities on the grit-blasted substrate surface being pulled off during failure and indicates a complex fracture path. Similar conclusions were reached for the GBS-pretreated steel joints.

The fact that the failure occurred mainly in the adhesive layer is consistent with the presence of covalent bonds being formed across

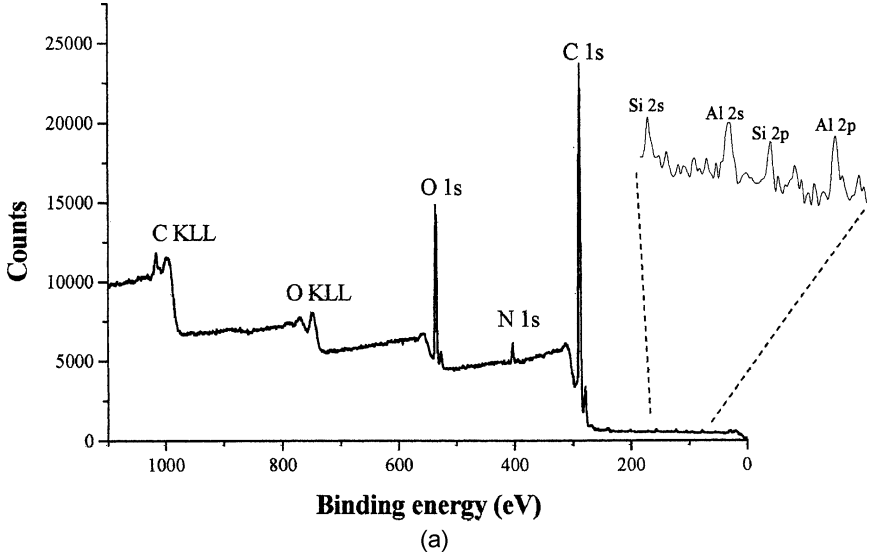

FIGURE 16 XPS spectra of a failed GBS-pretreated aluminium alloy joint: (a) adhesive side and (b) metal side (tested at 55% RH at a crack velocity of approximately 0.15 mm/min). (Continued).

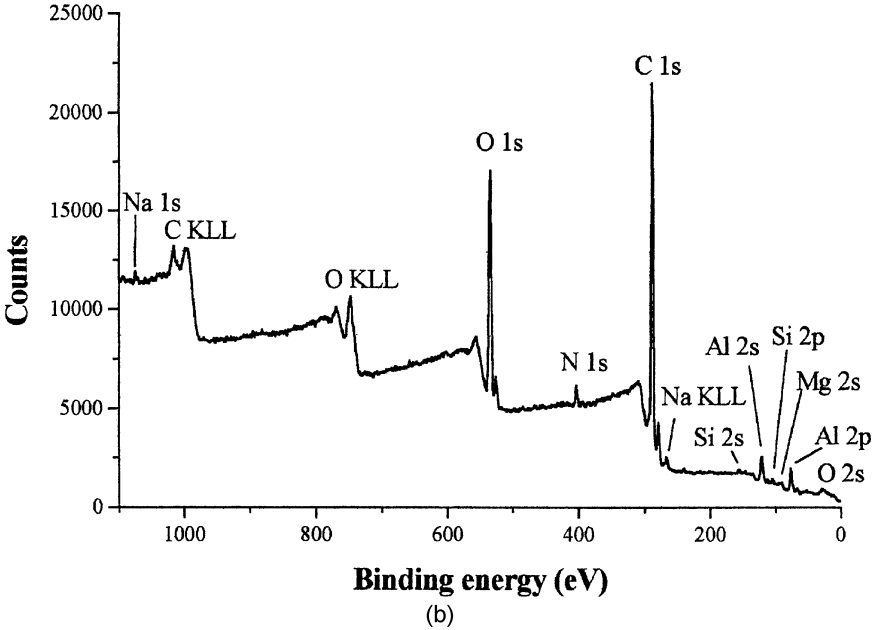

FIGURE 16 (Continued.)

the adhesive/substrate interface when a silane coupling agent is used, as is widely reported in the literature. As for the GBD-pretreated joints, it appears that the GBS-pretreated joints failed as a result of both the application of a stress and the presence of water molecules at the crack tip. As the RH was increased, the number of water molecules at the crack tip increased and the adhesive fracture energy decreased as a result, possibly due to the interfacial covalent bonds being attacked and ruptured. However, there is a clear suggestion that a critical concentration of water molecules may have to be attained in the case of the GBS surface-treated joints before any such environmental attack occurs (see Figure 10).

MECHANISMS OF FAILURE IN REGION III

Region III was observed at relatively high rates of displacement. In this region, the crack grew in a stick-slip manner, mainly cohesively in the adhesive layer, and the adhesive fracture energy, G_c, was relatively high. Indeed, as mentioned previously, the crack velocity was estimated to be equal to approximately 20 km/min. Furthermore,

the values of the adhesive fracture energy did not depend on the test environment but only on the surface pretreatment.

The fact that G_c was independent of the test environment and that the crack velocity was relatively high suggests that Region III corresponds to the situation when the rate of flow of water molecules to the crack tip is substantially slower than the rate of crack advance. Thus, the concentration of water molecules reaching the crack tip is below that needed for environmental attack on the interphase to occur. Hence, a relatively high value of G_c is recorded, with the locus of joint failure being mainly cohesively in the adhesive layer. This suggested mechanism is in agreement with similar work that has been previously reported on glass [7] and thermoplastic polymers [13, 14].

In Region III, the GBS-pretreated joints had a relatively high G_c value at crack initiation of 1010 ± 100 J/m^2, compared with the GBD joints where the value of G_c was 780 ± 100 J/m^2. However, it should be noted that the GBS-pretreated joints always failed completely in the adhesive layer. This is in contrast to the GBD-pretreated joints, where many of the joints exhibited some fraction of interfacial failure at the very point of crack initiation, with completely cohesive failure in the adhesive occurring as the crack propagated, at a relatively high velocity, down the TDCB specimen. However, the value of G_c for the GBD-pretreated joints was not significantly dependent upon the details of the locus of failure. This suggests that the difference in the values of the G_c for the GBD- and GBS-pretreated joints was not due to any minor difference in the locus of failure at crack initiation. The underlying reasons for these intriguing observations are discussed below.

THE TRANSITION FROM REGION I TO REGION III BEHAVIOUR

Maugis [25] has reviewed the transition from stable to stick-slip crack growth that occurs in brittle materials as the crack velocity is increased. To model the transition between stable (*i.e.*, our Region I behaviour) and unstable crack growth (*i.e.*, our Region III behaviour), he assumed that the log G_c *versus* log $\dot{a}$ curve observed experimentally was the result of the superposition of *two* curves, as shown schematically in Figure 17:

1. A curve corresponding to stable crack growth, *i.e.*, curve CAD, shows an increase in G_c with crack velocity governed by viscoelastic losses, followed by a decrease in G_c. The reason for this decrease is not clear, although this has been the subject of much debate. Maugis [25] has attributed the decrease in G_c after point "A" has

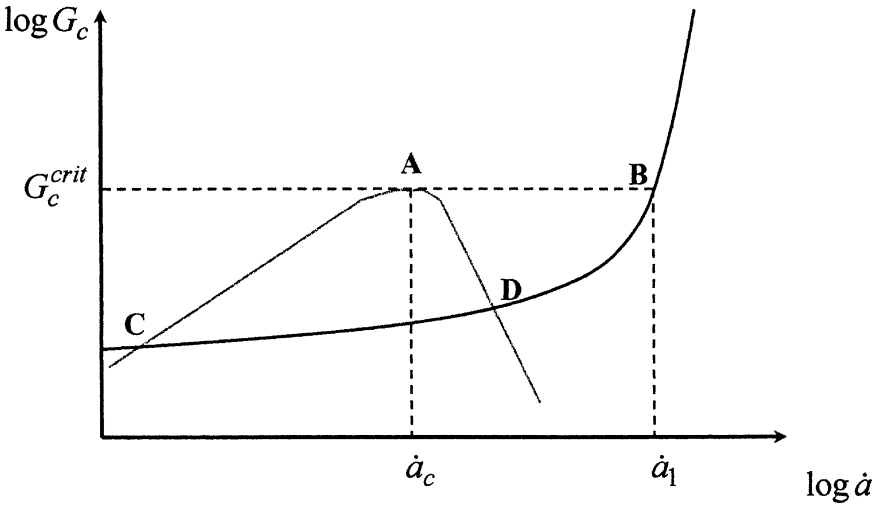

FIGURE 17 Schematic diagram showing the relationship between the fracture energy and crack velocity. The curve corresponding to stable (viscoelastic-controlled) crack growth is in light grey, whereas that corresponding to brittle fracture with dynamic effects is in black. Note that in this diagram the viscoelastic losses are schematically shown as being relatively large to highlight the transition, which is not the case for the present adhesive and is not a necessary requirement.

been reached to a significant reduction in the loss modulus, which occurs when the crack propagates sufficiently fast so that the material tends to behave in a more elastic fashion. On the other hand, Williams [14] has speculated that, for poly(methyl methacrylate), the decrease in G_c reported to occur between 1.5 m/min and 6 m/min (see Johnson and Radon [26], Williams [27], Marshall *et al.* [28], and Doll and Weidmann [29]) corresponded to the case where the heat generated at the crack tip is not dissipated, resulting in a softening of the polymer and a decrease in the fracture energy. Nonetheless, other workers [26] have suggested that the decrease in G_c is associated with a $\tan\delta_R$ peak, and that this $\tan\delta_R$ peak is governed by the β-process, *i.e.*, the viscoelastic relaxation corresponding to localised main-chain motions.

2. A second curve corresponding to purely "brittle" fracture with dynamic effects, *i.e.*, curve CDB. In this region, the crack velocity cannot exceed the Rayleigh velocity, which is the velocity of propagation of a stress wave travelling along a stress-free surface.

Now, for relatively low crack velocities, the initial dependence of fracture energy on crack velocity is governed by viscoelastic losses, and the portion CA of the curve CAD (Figure 17) is appropriate, *i.e.*, the portion of the curve CA is equivalent to Region I behaviour. However, when the rate of test is now increased by a small increment and the fracture energy becomes slightly greater than G_c^{crlt} (point A in Figure 17), the crack is forced to jump to the curve CDB and hence the crack velocity jumps suddenly from $\dot{a}_c$ to $\dot{a}_1$ (*i.e.*, point B is now attained). Thus, the essential argument is that the portion of the two curves ADB is not experimentally accessible, so that Region I behaviour is seen (curve CA) and is followed by Region III (point B).

However, in the present experiments, a further complication is that the transition from Region I to Region III behaviour is also accompanied by a change from visually interfacial failure to cohesive fracture through the adhesive layer. There are two factors that need to be considered which may possibly explain this accompanying change in the locus of failure. First, except at 0% RH, this change in the locus in failure upon going from Region I to Region III will arise, at least in part, from the lack of environmental attack and hence the lack of associated interfacial weakening that occurs in Region III. However, from Figure 8 it may be seen that this change in the locus of failure is also seen for the joints tested at 0% RH. Second, it is thus noteworthy that several groups of workers (*e.g.*, Wang and Suo [30], Fleck *et al.* [31], and Kinloch *et al.* [32]) have clearly shown that the locus of joint failure is not necessarily located where the joint may be at its weakest, *e.g.*, the plane where the value of $G_c$may be at its lowest. Instead, the locus of joint failure is governed by such factors as the values of G_c for the various potential failure paths coupled with the local strain-energy release rates, G, and stress fields available to initiate and propagate failure along these potential failure paths. For example, the above workers have shown that an increase in the shear stress component (*i.e.*, Mode II (in-plane shear) component) at an interfacial crack tip would tend to favour the crack kinking towards the center line of the adhesive layer. This arises since cracks always tend to favour growing along a pure Mode I (tensile) path. Now, interfacial cracks between materials possessing very different moduli and Poisson's ratios do have a significant shear stress component. In particular, Fleck *et al.* [31] have shown that for a crack in an adhesive joint a relatively very small change in the Mode I/Mode II ratio in the stress field at the crack tip can result in a change in the locus of failure from interfacial to cohesive in the adhesive layer. Thus, it is suggested that, as the value of G_c increases in the present TDCB joints upon going from Region I to Region III behaviour, the shear stress component

at the interfacial crack will increase and so cause the change from a visually interfacial to a cohesive (in the adhesive layer) locus of failure which is observed to accompany this change in behaviour.

Finally, we need to explain why the value of the adhesive fracture energy for stick-slip crack growth (*i.e.*, Region III) is higher for the GBS-pretreated joints than for the GBD-pretreated joints, as was noted earlier. According to Maugis [25], the G_c value on the "dynamic effects curve," *i.e.*, at point B, is dependent upon the G_c value in the stable regime of crack growth prior to the instability occurring (*i.e.*, the value of G_c at point A). Thus, if the portion of the curve CA, which corresponds to Region I stable crack growth, is shifted upwards, then the G_c value corresponding to point B (*i.e.*, Region III behaviour) will also increase.

CONCLUSIONS

In the present study the adhesive fracture energy, G_c, of aluminium alloy and steel joints bonded using a rubber-toughened epoxy has been measured *via* a fracture mechanics approach employing tapered double-cantilever beam (TDCB) joints that were loaded monotonically. The substrates were either (1) grit-blasted and degreased (GBD) or (2) silane (GBS) pretreated. The monotonically loaded tests were undertaken over a wide range of constant rates of displacement, $\dot{y}$, of the crosshead and at different levels of RH. The adhesive fracture energy, G_c, was determined as a function of the crack velocity, $\dot{a}$. When the data were plotted in the form of $\log_{10} G_c$ *versus* $\log_{10} \dot{a}$, three clearly different regions of crack growth behaviour could be identified, and these have been labelled "Region I," "Region II," and "Region III."

Region I

At slow crack velocities, the value of the adhesive fracture energy, G_c, was relatively low and the crack grew visually along the adhesive/substrate interface. The value of G_c was almost constant with increasing crack velocity, and the dependence of G_c upon the crack velocity, $\dot{a}$, was controlled by the viscoelastic nature of the epoxy adhesive. The low dependence of the value of G_c upon the crack velocity was attributed to the low value of the viscoelastic loss factor of the epoxy adhesive in this range, arising from the highly crosslinked structure of the epoxy polymer. The G_c value was observed to decrease linearly with the RH, since water molecules were readily able to reach the crack tip and to attack the interface. However, especially for the GBS-pretreated joints, one could infer that a critical RH, below which

interfacial attack and weakening of the joints did not occur, might well exist. Further, the use of the silane pretreatment was clearly successful in increasing the value of the adhesive fracture energy, G_c. The improvement in joint durability observed in this Region I when using the silane primer was considered to arise from the formation of covalent bonds between the substrates and the adhesive.

Region III

The crack velocity was constant and estimated to be equal to approximately 20 km/min. The crack grew in a stick-slip manner with relatively high values of fracture energy at crack initiation. No water molecules were considered to be able to reach the crack tip, since the environment had no effect on the value of G_c. The crack grew mainly cohesively in the adhesive layer, possibly because the shear stress component of the local stress field at the crack tip was sufficiently high so as to force the crack to kink towards the centre of the adhesive layer. In this region, the GBS-pretreated joints had a higher G_c value at crack initiation than the GBD-pretreated joints due to the higher intrinsic adhesion achieved when employing the silane pretreatment.

Region II

Between Region I and Region III two types of transition regions were observed, termed either "Region IIa" or "Region IIb." In Region IIa the crack grew stably along the interface, and the value of G_c increased sharply before the crack propagated cohesively in the adhesive layer in a stick-slip manner (*i.e.*, Region III was attained). The crack velocity (corresponding to the sharp increase in G_c) was considered to be equivalent to the rate of water molecules flowing to the crack tip. When the crack velocity was somewhat higher than the rate of the flow of water molecules to the crack tip, then the concentration of water molecules at the crack tip would be insufficient to cause interfacial attack and weakening. Hence, the value of G_c now increased sharply to give Region III behaviour. In Region IIb, only a change in the type of crack growth was observed (*i.e.*, from stable (interfacial) crack growth in Region I to unstable, slip-stick (cohesively in the adhesive) crack growth in Region III), with no sharp increase in G_c being observed as in Region IIa.

REFERENCES

[1] Kinloch, A. J., Ed., *Durability of Structural Adhesives* (Applied Science, London and New York, 1983).
[2] Davies, R. J. and Kinloch, A. J., In: *Adhesion 13*, Allen, K. W. (Ed.) (Elsevier, London, 1988), pp. 8–21.
[3] Jethwa, J. K. and Kinloch, A. J., *J. Adhesion* **61**, 71–95 (1997).
[4] Curley, A. J., Hadavinia, H., Kinloch, A. J., and Taylor, A. C., *Int. J. Fract.* **103**, 41–69 (2000).
[5] Digby, R. P. and Shaw, S. J., *Int. J. Adhesion Adhesives* **18**, 261–264 (1998).
[6] O'Brien, F. E. M., *J. Sci. Instruments* **25**, 73–76 (1948).
[7] Wiederhorn, S. M., *J. Am. Ceram. Soc.* **50**, 407–414 (1967).
[8] Blackman, B. R. K., Hadavinia, H., Kinloch, A. J., Paraschi, M., and Williams, J. G., *Eng. Fract. Mech.* **70**, 233–248 (2003).
[9] Gledhill, R. A. and Kinloch, A. J., *J. Mater. Sci. Lett.* **10**, 1261–1263 (1975).
[10] Arnott, D. R. and Kindermann, M. R., *J. Adhesion* **48**, 85–100 (1995).
[11] Gledhill, R. A., Kinloch, A. J., and Shaw, S. J., *J. Adhesion* **11**, 3–15 (1980).
[12] Brewis, D. M., Comyn, J., Raval, A. K., and Kinloch, A. J., *Int. J. Adhesion Adhesives* **10**, 247–253 (1990).
[13] Williams, J. G. and Marshall, G. P., *Proc. R. Soc. Lond.* **A 342**, 55–57 (1975).
[14] Williams, J. G., *Fracture Mechanics of Polymers* (Ellis Horwood Ltd, Chichester, 1984), pp. 175–235.
[15] Gledhill, R. A., Kinloch, A. J., Yamini, S., and Young, R. J., *Polymer* **19**, 574–582 (1978).
[16] Kavanagh, G. M. and Tod, D. A., in *Proceedings of the Euradh 2002-Adhesion '02 Conference*, Glasgow, UK (Institute of Materials, London, 2002), pp. 100–104.
[17] Gledhill, R. A. and Kinloch, A. J., *J. Adhesion* **6**, 315–330 (1974).
[18] Kinloch, A. J., Dukes, W. A., and Gledhill, R. A., *Adhesion Science and Technology* Vol. B, (Plenum Press, New York, 1975), pp. 597–614.
[19] Gettings, M., Baker, F. S., and Kinloch, A. J., *J. Applied Polymer Sci.* **21**, 2375–2392 (1977).
[20] Yahalom, J.,and Aladjem, A., Eds., *Stress Corrosion Cracking* (Freund, Tel Aviv, 1980).
[21] Gettings, M. and Kinloch, A. J., *J. Mater. Sci.* **12**, 2511–2518 (1977).
[22] Plueddeman, E. P., *Silane Coupling Agents* (Plenum Press, New York, 1982).
[23] Davis, S. J. and Watts, J. F., *Int. J. Adhesion Adhesives* **16**, 5–15 (1996).
[24] Abel, M.-L., Digby, R. P., Fletcher, I. W., and Watts, J. F., *Surface and Interface Analysis* **29**, 115–125 (2000).
[25] Maugis, D., *J. Mater. Sci.* **20**, 3041–3073 (1980).
[26] Johnson, F. A. and Radon, J. C., *Eng. Fract. Mech.* **4**, 555–576 (1972).
[27] Williams, J. G., *Int. J. Fract. Mech.* **8**, 393–401 (1972).
[28] Marshall, G. P., Coutts, L. H., and Williams, J. G., *J. Mater. Sci.* **9**, 1409–1419 (1974).
[29] Doll, W. and Weidmann, G. W., *J. Mater. Sci. Lett.* **11**, 2348–2350 (1976).
[30] Wang, J. S. and Suo, Z., *Acta Metall. Mater.* **38**, 1279–1290 (1990).
[31] Fleck, N. A., Hutchinson, J. W., and Suo, Z., *Int. J. Solids and Structures* **27**, 1683–1703 (1991).
[32] Kinloch, A. J., Thrusabanjong, E., and Williams, J. G., *J. Mater. Sci.* **26**, 6260–6270 (1991).